

Chen, T.-W., Vervoort, J. D., and Baldwin, J. A., 2023, Growth and evolution of Neoarchean–Paleoproterozoic crust in the NW Wyoming Province: Evidence from zircon U-Pb age and Lu-Hf isotopes of the Montana metasedimentary terrane: GSA Bulletin, <https://doi.org/10.1130/B37160.1>.

Supplemental Material

Table S1. Metadata for laser data.

Table S2. Summary of U-Pb isotope for zircon reference materials.

Table S3. Summary of Lu-Hf isotope for zircon reference materials.

Table S4. Summary of U-Pb isotope for zircon samples.

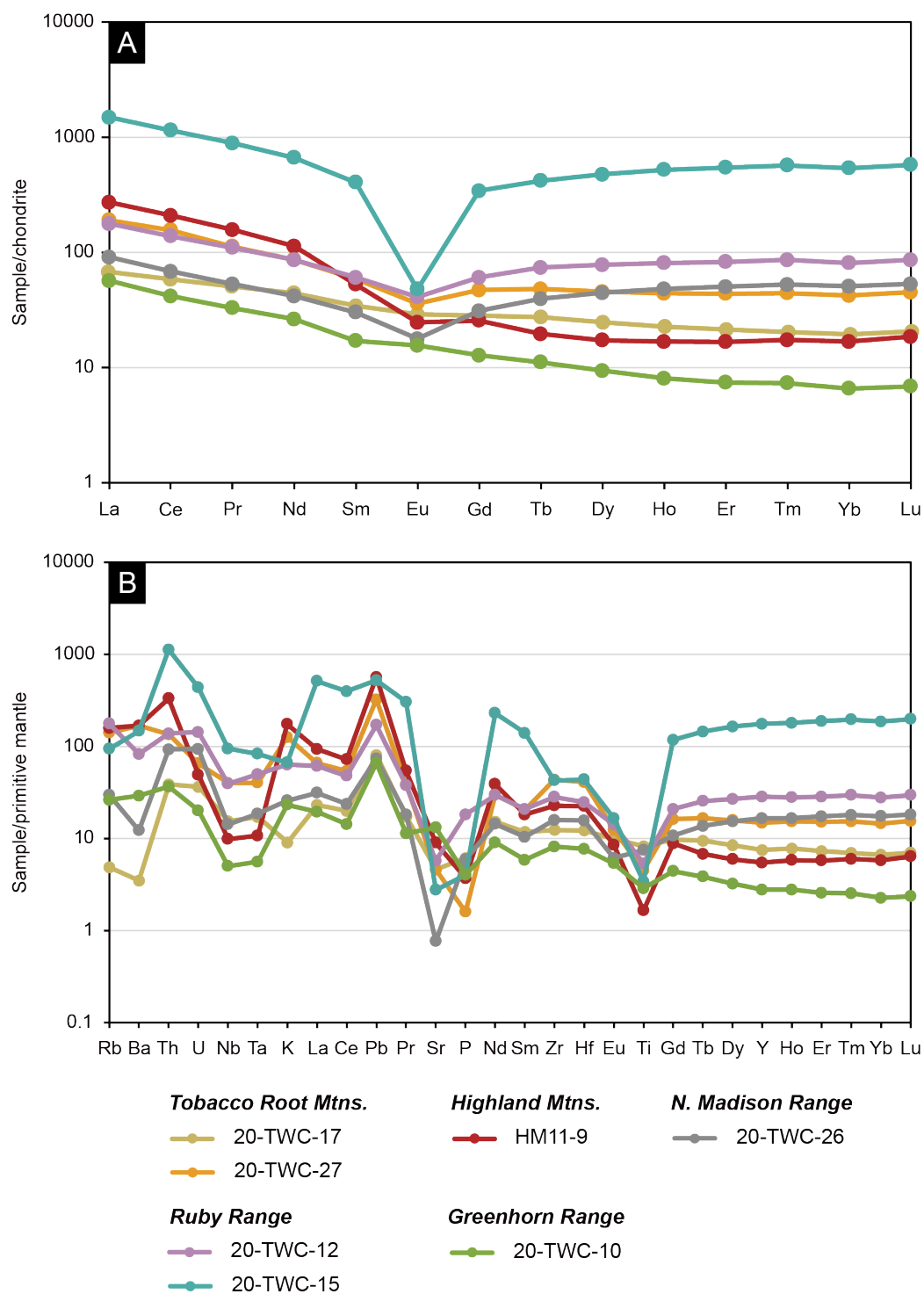
Table S5. Summary of Lu-Hf isotope for zircon samples.

Table S6. Whole-rock major- and trace-element compositions.

Figure S1. Whole-rock trace-element diagrams.

Supplemental File S1. Sample description.

Supplemental File S2. Whole-rock chemistry.



1

2 **Figure S1.** Whole-rock trace-element diagrams of seven metaigneous samples. (A) Chondrite
 3 normalized REE patterns. (B) Primitive mantle normalized multi-element diagrams. Chondrite
 4 and primitive mantle compositions are from Sun and McDonough (1989).

5 **REFERENCES CITED**

- 6 Sun, S.-S., and McDonough, W. F., 1989, Chemical and isotopic systematics of oceanic basalts:
7 implications for mantle composition and processes: Geological Society, London, Special
8 Publications, v. 42, no. 1, p. 313-345.

1 **Supplemental File S1: Sample description**

2 Here we provide the rock description, mineral assemblage, and zircon internal structures of each
3 sample.

4 ***Tobacco Root Mountains***

5 *20-TWC-17*

6 This sample was collected from the Thompson Peak. It is a moderately-to-strongly foliated and
7 medium grained amphibolite with few quartz veins. The mineral assemblage includes amphibole,
8 garnet, plagioclase, as well as accessory mineral phases of apatite and zircon. This sample has a
9 low yield of zircon grains due to its mafic composition (Table S6). The zircon grains are average
10 ~100 μm in length and are subhedral in form. The internal textures show no visual evidence of
11 inherited cores or metamorphic overgrowths. Some grains display irregular and patchy zoning
12 (e.g., Fig. 3.2), while others lack visible zoning (e.g., Fig. 3.6).

13 *20-TWC-27*

14 This sample was collected from the Virginia Creek Road. It is a strongly foliated and fine-to-
15 medium grained quartzofeldspathic gneiss. The mineral assemblage includes biotite, garnet,
16 microcline feldspar, plagioclase, quartz, as well as accessory mineral phases of apatite and
17 zircon. Zircon grains are generally over 250 μm in length and have euhedral crystal forms. Most
18 zircon grains preserve oscillatory zoning. Some grains display core-overgrowth relationships
19 (e.g., Fig. 3.11).

20 ***Highland Mountains***

21 *HM11-9*

22 This sample was collected from the Camp Creek Road. It is a moderately foliated and massive
23 medium grained granitic gneiss. The mineral assemblage includes biotite, garnet, microcline

feldspar, quartz, as well as accessory mineral phases of apatite, monazite, and zircon. Zircon grains typically have lengths over 250 μm and have elongated prismatic crystal forms. The internal textures show no visual evidence of inherited cores. Most of zircon grains preserve oscillatory zoning (e.g., Fig. 3.16), a typical feature of magmatic zircon.

Northern Madison Range

20-TWC-26

This sample was collected from the Bear Trap Canyon. It is a moderately foliated and medium grained gneiss. The mineral assemblage is characterized by abundant gedrite and garnet and contains plagioclase, quartz, as well as accessory mineral phases of apatite and zircon. This sample has a low yield of zircon grains due to its mafic composition (Table S6). Zircon grains are generally 100 μm in length and have a subhedral crystal form. CL images show two distinct domains: the brighter domain (dated at ~ 1.8 Ga) shows concentric zoning (e.g., Fig. 3.22), while the darker domain (dated at ~ 2.4 Ga) shows weak sector zoning (e.g., Fig. 3.23). Figure 3 illustrates one case where a darker domain is overgrown by a brighter domain (Fig. 3.25).

Ruby Range

20-TWC-12

This sample was collected from Cottonwood Creek Road. It is a weakly-to-moderately foliated and medium grained amphibolite with subordinate quartz veins. The mineral assemblage includes amphibole, garnet, as well as accessory mineral phases of apatite, zircon, and sparse titanite. Zircon grains are generally over 200 μm in length and show a subhedral-to-euhedral crystal form. A few grains display weak concentric zoning (e.g., Fig. 3.29), while others lack visible zoning (e.g., Fig. 3.31). Some grains display core-overgrowth relationships (e.g., Fig. 3.28).

47 *20-TWC-15*

48 This sample was collected from Cottonwood Creek Road. It is a weakly foliated and medium
49 grained leucocratic gneiss. The mineral assemblage includes garnet, microcline feldspar, quartz,
50 as well as accessory mineral phases of apatite, monazite, and zircon. Zircon grains are ~250 µm
51 in length and have subhedral-to-euhedral crystal forms. These grains are all metamict and it is
52 difficult to observe their crystalline structures by CL images (Figs. 3.35-3.40).

53 ***Greenhorn Range***

54 *20-TWC-10*

55 This sample was collected from Barton Gulch. It is a weakly foliated and coarse-grained
56 amphibolite. The mineral assemblage includes amphibole, plagioclase, garnet, as well as
57 accessory mineral phases of apatite, titanite, and zircon. Zircon grains generally have long-axis
58 lengths over 100 µm with subhedral crystal forms. The internal textures show no visual evidence
59 of inherited cores or metamorphic overgrowths. Some grains display sector zoning (e.g., Fig.
60 3.43), and a few grains show fine oscillatory-zoned bands (e.g., Fig. 3.41).

61 **Supplemental File S2: Whole-rock chemistry**

62 Whole-rock major- and trace-element data are given in Table S6. The REE pattern (normalized
63 to chondrite compositions, Sun and McDonough, 1989) and multi-element diagram (normalized
64 to primitive mantle compositions, Sun and McDonough, 1989) are shown in Figure S1.

65 Rock samples were crushed, chipped, and ground into powders in the GeoAnalytical Laboratory
66 (GAL) at Washington State University (WSU). Rock powders were mixed with a flux, dilithium
67 tetraborate ($\text{Li}_2\text{B}_4\text{O}_7$), in a weight ratio of 2:1. The mixed powders were placed into graphite
68 crucibles and fused for 10 minutes at 1000°C in a muffle furnace. After fully cooled down, the
69 sample powders formed glass beads. Each bead was reground into glass powders for
70 homogeneity. To analyze major elements by the X-ray fluorescence spectrometer, the glass
71 powders had to be replaced into graphite crucibles and refused for 10 minutes at 1000°C.

72 Following the second fusion, the cooled beads were polished and rinsed with alcohol to remove
73 surficial contaminations.

74 Ten major and twenty-seven selected trace elements for bulk rocks were analyzed at the WSU
75 GAL. For the trace-element analysis, the glass powders were digested twice in acid mixture of
76 HF, HNO_3 , and HClO_4 at 110°C and 160°C. The dissolution with HF quantitatively removed
77 silica and flux as gaseous fluorides. Following two times of evaporation, samples were brought
78 into HNO_3 and diluted with deionized water, then were ready to be analyzed by ICPMS. Detailed
79 procedures for major- and trace-element analyses are described in Johnson et al. (1999) and
80 Knaack et al. (1994), respectively.

81 ***Tobacco Root Mountains***

82 *20-TWC-17*

This sample has composition that falls within the range of basic rocks with low SiO₂ content (48.94 wt%) and relatively high MgO content (7.03 wt%). The low yield of zircon grains for this sample is consistent with the mafic original composition. In the REE pattern and multi-element diagram (Fig. S1), it is characterized by slight enrichment in light REE ((La/Sm)_N = 1.96) relative to heavy REE ((Gd/Lu)_N = 1.38), with weak or no depletion in Eu (Eu/Eu* = 0.92) and high field strength elements (HFSEs: Nb, Ta, and Ti).

20-TWC-27

This sample has composition that falls within the range of acidic rocks with high SiO₂ content (71.47 wt%) and very low MgO content (0.09 wt%). In the REE pattern and multi-element diagram (Fig. S1), it is characterized by enrichment in light REE ((La/Sm)_N = 3.24) relative to heavy REE ((Gd/Lu)_N = 1.04) and enrichment in large ion lithophile elements (LILEs: Rb and Ba), with depletion in Eu (Eu/Eu* = 0.68) and HFSEs (Nb, Ta, and Ti).

Highland Mountains

HM11-9

This sample has composition that falls within the range of acidic rocks with high SiO₂ content (73.24 wt%) and low MgO content (0.83 wt%). In the REE pattern and multi-element diagram (Fig. S1), it is characterized by significant enrichment in light REE ((La/Sm)_N = 5.16) relative to heavy REE ((Gd/Lu)_N = 1.38), with depletion in Eu (Eu/Eu* = 0.63) and HFSEs (Nb, Ta, and Ti).

Northern Madison Range

20-TWC-26

This sample has composition that falls within the range of basic rocks with low SiO₂ content (50.95 wt%) and relatively high MgO content (7.66 wt%). The low yield of zircon grains for this

sample is consistent with the mafic original composition. In the REE pattern and multi-element diagram (Fig. S1), it is characterized by mild enrichment in light REE ($(\text{La}/\text{Sm})_{\text{N}} = 3.01$) relative to heavy REE ($(\text{Gd}/\text{Lu})_{\text{N}} = 0.59$) and depletion in Eu ($\text{Eu}/\text{Eu}^* = 0.58$), with weak or no depletion in HFSEs (Nb, Ta, and Ti).

Ruby Range

20-TWC-12

This sample has composition that falls within the range of intermediate rocks with SiO_2 content of 63.75 wt% and MgO content of 1.29 wt%. In the REE pattern and multi-element diagram (Fig. S1), it is characterized by mild enrichment in light REE ($(\text{La}/\text{Sm})_{\text{N}} = 2.93$) relative to heavy REE ($(\text{Gd}/\text{Lu})_{\text{N}} = 0.68$), with depletion in Eu ($\text{Eu}/\text{Eu}^* = 0.68$) and HFSEs (Nb, Ta, and Ti).

20-TWC-15

This sample has composition that falls within the range of intermediate rocks with SiO_2 content of 62.15 wt% and MgO content of 1.74 wt%. In the REE pattern and multi-element diagram (Fig. S1), it is characterized by high concentrations of trace elements, with enrichment in light REE ($(\text{La}/\text{Sm})_{\text{N}} = 3.66$) relative to heavy REE ($(\text{Gd}/\text{Lu})_{\text{N}} = 0.59$) and significant depletion in Eu ($\text{Eu}/\text{Eu}^* = 0.13$) and HFSEs (Nb, Ta, and Ti).

Greenhorn Range

20-TWC-10

This sample has composition that falls within the range of intermediate rocks with SiO_2 content of 59.10 wt% and MgO content of 4.06 wt%. In the REE pattern and multi-element diagram (Fig. S1), it is characterized by enrichment in light REE ($(\text{La}/\text{Sm})_{\text{N}} = 3.32$) relative to heavy REE ($(\text{Gd}/\text{Lu})_{\text{N}} = 1.86$) and depletion in HFSEs (Nb, Ta, and Ti), with slightly positive Eu anomaly ($\text{Eu}/\text{Eu}^* = 1.04$).

129 **REFERENCES CITED**

- 130 Johnson, D. M., Hooper, P. R., and Conrey, R. M., 1999, XRF Analysis of rocks and minerals
131 for major and trace elements on a single low dilution Li-tetraborate fused bead: Advances
132 in X-rays Analysis, v. 41, p. 843-867.
- 133 Knaack, C., Cornelius, S., and Hooper, P. R., 1994, Trace element analyses of rocks and
134 minerals by ICP-MS: Open File Report, Department of Geology, Washington State
135 University.
- 136 Sun, S.-S., and McDonough, W. F., 1989, Chemical and isotopic systematics of oceanic basalts:
137 implications for mantle composition and processes: Geological Society, London, Special
138 Publications, v. 42, no. 1, p. 313-345.